THE JOURNAL OF BIOLOGICAL CHEMISTRY VOL. 281, NO. 6, pp. 3329–3334, February 10, 2006

Mutations in the Amino Terminus of the Cystic Fibrosis Transmembrane Conductance Regulator Enhance Endocytosis*

Received for publication, July 25, 2005, and in revised form, November 22, 2005 Published, JBC Papers in Press, December 8, 2005, DOI 10.1074/jbc.M508131200

Asta Jurkuvenaite[‡], Karoly Varga[‡**], Krzysztof Nowotarski[§**], Kevin L. Kirk[§**], Eric J. Sorscher[¶**], Yao Li[‖**], John P. Clancy[‖**], Zsuzsa Bebok[‡**], and James F. Collawn[‡**1]**

*From the Departments of [‡]Cell Biology, [§]Physiology and Biophysics, [¶]Medicine, [‖]Pediatrics, and the **Gregory Fleming James Cystic Fibrosis Center, University of Alabama at Birmingham, Birmingham, Alabama 35294*

Efficient endocytosis of the cystic fibrosis transmembrane conductance regulator (CFTR) is mediated by a tyrosine-based internalization signal in the CFTR carboxyl-terminal tail ^{1424}YDSI^{1427}. In the present studies, two naturally occurring cystic fibrosis mutations in the amino terminus of CFTR, R31C, and R31L were examined. To determine the defect that these mutations cause, the Arg-31 mutants were expressed in COS-7 cells and their biogenesis and trafficking to the cell surface tested in metabolic pulse-chase and surface biotinylation assays, respectively. The results indicated that both Arg-31 mutants were processed to band C at ~50% the efficiency of the wild-type protein. However, once processed and delivered to the cell surface, their half-lives were the same as wild-type protein. Interestingly, indirect immunofluorescence and cell surface biotinylation indicated that the surface pool was much smaller than could be accounted for based on the biogenesis defect alone. Therefore, the Arg-31 mutants were tested in internalization assays and found to be internalized at 2× the rate of the wild-type protein. Patch clamp and 6-methoxy-*N*-(3-sulfopropyl)quinolinium analysis confirmed reduced amounts of functional Arg-31 channels at the cell surface. Together, the results suggest that both R31C and R31L mutations compromise biogenesis and enhance internalization of CFTR. These two additive effects contribute to the loss of surface expression and the associated defect in chloride conductance that is consistent with a disease phenotype.

The cystic fibrosis transmembrane conductance regulator (CFTR)[2] is the chloride channel that is defective in cystic fibrosis. CFTR is found at the apical surface of a number of epithelial cell types and is known to undergo endocytosis (1, 2) through clathrin-coated vesicles (2, 3). Further, it has been suggested that CFTR internalization may provide a mechanism for controlling the cyclic AMP-stimulated chloride channel activity at the cell surface (2). The internalization and recycling pathways of cell surface CFTR suggest that significant amounts of CFTR are found within the endocytic pathway, and this is consistent with a number of studies in different cell types (4–9).

CFTR endocytosis is mediated by a tyrosine-based signal, ^{1424}YDSI^{1427}, in the carboxyl-terminal cytoplasmic tail of CFTR (10–12). This sequence conforms to a consensus internalization signal that consists of *YXX*Φ, where Φ is a large hydrophobic residue and *X* is any residue (13). This sequence, YDSI, has been shown to interact with the μ2 subunit of the AP-2 adaptor complex (14–16). Alanine substitutions of the tyrosine and isoleucine residues result in an accumulation of the double alanine mutant CFTR at the cell surface, with a matching increase in chloride channel function (12). Interestingly, loss of the signal has no effect on the protein half-life, suggesting that internalization is not the rate-limiting step for CFTR degradation.

Over 1400 mutations have been identified in the *CFTR* gene, and these are classified into six classes (reviewed in Ref. 17). Class II mutations that affect protein maturation are the most prevalent, and the prototype of this class, ΔF508, is the most common disease-causing mutation. This mutation confers a temperature-sensitive folding defect (18); when cell lines expressing this protein are cultured at 27 °C for 2 days, ΔF508 CFTR is released to the cell surface (18), where it reduces single channel activity (20). Interestingly, even after delivery to the cell surface, ΔF508 is rapidly down-regulated (21), suggesting multiple defects that need to be corrected to restore normal chloride channel function. Therefore, identification of the structural features in CFTR responsible for proper cell surface trafficking are of great interest.

In the present studies, we examined two naturally occurring mutations, R31C and R31L, which cause mild CF.[3] To determine the defects caused by these missense mutations, we expressed them in COS-7 cells and analyzed their biogenesis and trafficking. Our results indicate that both R31C and R31L have compromised biogenesis and enhanced endocytosis compared with wild-type CFTR. These two additive defects contribute to the low surface expression of the mutants. Patch clamp studies confirmed the biochemical data and showed a dramatic decrease in the functional surface pool of both Arg-31 CFTR mutants.

MATERIALS AND METHODS

Construction of CFTR Mutants—The R31C and R31L mutants were prepared by PCR mutagenesis. Cloning vectors, oligos, enzymes, and reagents were from Invitrogen. PCR reactions were performed using Platinum Pfx polymerase according to the manufacturer's suggested protocol. Using the *CFTR* gene contained in plasmid pCDNA3.1+ as template, the R31L and R31C mutants were constructed by PCR-mutagenesis using a pair of internal primers for each mutant, annealing at the Arg-31 coding site, and a pair of external primers, one annealing at the Nhe-I site of the multilinker of the vector, and one annealing at the BspE-I site in the CFTR gene. The oligos used were (5′–3′): CFTR_R31L(+), GAGGAAAGGATACAGACAGCTCCTGGAATT-

* This work was supported by grants from the National Institutes of Health (DK60065 to J. F. C.; HL076587 to Z. B.), and by a Cystic Fibrosis Foundation Research Development Program grant (to E. J. S.). The costs of publication of this article were defrayed in part by the payment of page charges. This article must therefore be hereby marked "*advertisement*" in accordance with 18 U.S.C. Section 1734 solely to indicate this fact.

[1] To whom correspondence should be addressed: Dept. of Cell Biology, University of Alabama at Birmingham, 1918 University Blvd., MCLM 350, Birmingham, AL 35294. Tel.: 205-934-1002; Fax: 205-975-5648; E-mail: jcollawn@uab.edu.

[2] The abbreviations used are: CFTR, cystic fibrosis transmembrane conductance regulator; CF cystic fibrosis; TES, *N*-tris(hydroxymethyl)methyl-2-aminoethanesulfonic acid; SPQ, 6-methoxy-*N*-(3-sulfopropyl)quinolinium; MgATP, magnesium adenosine triphosphate.

[3] CF Genetic Analysis Consortium, www.genet.sickkids.on.ca/cftr.

GTCAGACATATAC; CFTR_R31L(−), GTATATGTCTGACAATTCCAGGAGCTGTCTGTATCCTTTCCTC; CFTR_R31C(+), GAGGAAAGGATACAGACAGTGCCTGGAATTGTCAGACATATAC; CFTR_R31C(−), GTATATGTCTGACAATTCCAGGCACTGTCTGTATCCTTTCCTC; PCDNA-Nhe-N, GGCTAGCGTTTAAACTTAAGC; and CFTR-BspEI-C, GAATATTTTCCGGAGGATGATTC.

For each mutation, a pair of PCR reactions was performed, one using the external N primer and the internal (−) primer, another using the external C primer and the internal (+) primer. An aliquot from each reaction was then combined in a second reaction with both external primers. Annealing at, and extension from, the homologous termini of the first reaction products provided the template for the second reaction. The products of the second reactions were cloned using the PCR cloning vector pCR-Blunt. Mutant clones were verified by DNA sequence analysis (University of Alabama at Birmingham, Center for AIDS Research/Comprehensive Cancer Center Sequencing Core) and subcloned back into the CFTR gene in pCDNA3.1+ at the Nhe-I and BspE-I sites.

Cell Culture and Transient Transfection of COS-7 Cells—COS-7 cells were obtained from the American Type Culture Collection (ATCC) (Manassas, VA). The cells were cultured as described previously (10) and transiently transfected using Lipofectamine Plus reagent (Invitrogen) according to the manufacturer's directions. Transfection efficiencies were monitored by co-transfection with green fluorescent protein and generally approximated 60%. The cells were incubated at 37 °C in a humidified incubator for 48 h before analysis.

Immunoprecipitation of CFTR—One T75 flask of confluent-transfected COS-7 cells was used 48 h post-transfection. The cells were lysed in radioimmune precipitation assay buffer containing a protease inhibitor mixture (Roche Diagnostics). CFTR was immunoprecipitated using a mouse monoclonal anti-carboxyl-terminal tail 24–1 antibody (ATCC number HB-11947) coupled to protein A-agarose (Roche Diagnostics) (22).

Metabolic Pulse-Chase Assays—These experiments were performed as described previously (22) and analyzed by SDS-PAGE and autoradiography (PhosphorImager, Amersham Biosciences). Calculation of protein half-lives was performed as described by Straley *et al.* (23). Maturation efficiency was measured by comparing the density of the labeled immature, core-glycosylated form (B band) to the density of the fully glycosylated protein (C band) using IPLab software (Scanalytics, Inc.) (24).

Cell Surface Biotinylation—Cell surface glycoproteins were biotinylated using previously established methods (12) with the following modifications. Briefly, after surface biotinylation with biotin LC hydrazide, the cells were lysed in radioimmune precipitation assay buffer with a protease inhibitor mixture (30 min on ice), and CFTR was immunoprecipitated with a monoclonal antibody to CFTR (24–1) coupled to protein A-agarose. CFTR was eluted from the beads with 2× Laemmli sample buffer, run on SDS-PAGE gels, and transferred to polyvinylidene difluoride membranes (Bio-Rad). Biotinylated CFTR was detected with horseradish peroxidase-labeled avidin. Chemiluminescence was induced with Pico Super Signal peroxide solution (Pierce). The membranes were exposed for different time periods up to 1 min, and a linear range for a standard set of diluted samples was calibrated.

Endocytosis Assays—Internalization assays were performed as described previously with minor modifications (10, 12). Biotinylated CFTR was detected using Western blot analysis after calibration of a standard curve of diluted samples. CFTR internalization was detected as percentage of loss of biotinylated CFTR in the 2.5-min warm-up period compared with the control samples (no warm-up period).

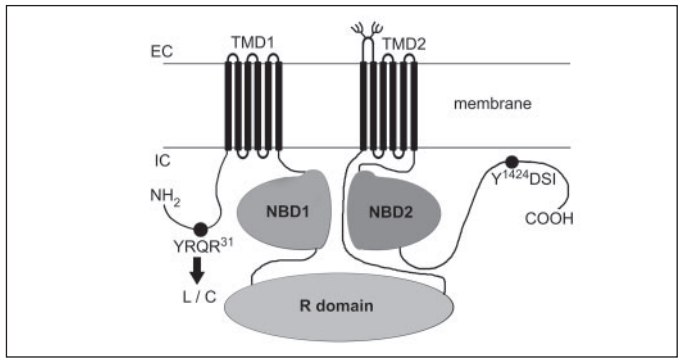

FIGURE 1. **Schematic diagram of CFTR.** The CFTR molecule consists of 2 transmembrane-spanning domains (*TMD1* and *TMD2*), two cytoplasmic nucleotide-binding domains (*NBD1* and *NBD2*), a regulatory domain (*R*), and amino- and carboxyl-terminal cytoplasmic tails. CFTR has an internalization signal in its carboxyl-terminal tail that consists of ^{1424}YDSI^{1427} (Peter *et al.* (12)). This motif conforms to the Y*XX*Φ motif first identified for tyrosine-based internalization signals, where Φ is a large hydrophobic residue and *X* is any residue (13). *EC*, extracellular; *IC*, intracellular; *L/C*, R31L and R31C mutations.

Microscopy—Indirect immunofluorescence was performed as described previously (24).

Patch Clamp Analysis—Macroscopic currents were recorded in the excised, inside-out configuration. Patch pipettes were pulled from Corning 8161 glass to tip resistances of 3 megohms. CFTR channels were activated following patch excision by exposure of the cytoplasmic face of the patch to the catalytic subunit of protein kinase A (110 units/ml; Promega) and MgATP (1 mM). Currents were recorded in symmetrical solutions containing (in mM): 140 *N*-methyl-D-glucamine-Cl, 3 $MgCl_2$, 1 EGTA, and 10 TES, pH 7.3. Macroscopic currents were evoked using a ramp protocol from +80 to −80 mV with a 4-s time period. Signals from macroscopic recording were filtered at 20 Hz. Data acquisition and analysis were performed using pCLAMP 9.1 software (Axon Instruments). All patch clamp experiments were performed at 21–23 °C.

SPQ Fluorescence Assays—CFTR function in individual cells was assayed using the halide-quenched dye SPQ (25). Briefly, cells were loaded for 10 min with SPQ (10 mM) by hypotonic shock and then mounted in a specially designed perfusion chamber for fluorescence measurements. Fluorescence (*F*) of single cells was measured with a Zeiss inverted microscope, a PTI imaging system, and a Hamamatsu camera. Excitation was at 340 nm, and emission was >410 nm. All functional studies were conducted at 23 °C. Base-line fluorescence was measured in isotonic NaI buffer (NaI buffer; 130 mM NaI, 5 mM KNO_3, 2.5 mM $Ca(NO_3)_2$, 2.5 mM $Mg(NO_3)_2$, 10 mM D-glucose, 10 mM HEPES) followed by perfusion with isotonic dequenching buffer ($NaNO_3$ replaced NaI) to measure unregulated efflux and then $NaNO_3$ buffer with 20 μM forskolin as indicated. At the end of each experiment, the cells were returned to the NaI buffer for requenching (1100 s). The increase in fluorescence above the basal (NaI-quenched) level is shown (% increase $F >$ basal) (Fig. 6*E*). The data are cumulative from three coverslips in each condition studied in a paired fashion on three separate days ($n = 120$ cells/curve). The bottom 10% of cells in all conditions (attributable to inadequate SPQ loading, cell detachment, etc.) were discarded, and the data obtained from the top 90% of cells in each condition were analyzed as previously described (26, 27). Wild-type CFTR-expressing cells had an increased dequenching in NO_3 buffer and NO_3 buffer plus forskolin, as previously described, presumably because of varying levels of wild-type CFTR activation.

Statistical Analysis—Results were expressed as means ± S.D. Statistical significance among means was determined using the Student's *t* test (two samples) unless otherwise indicated.

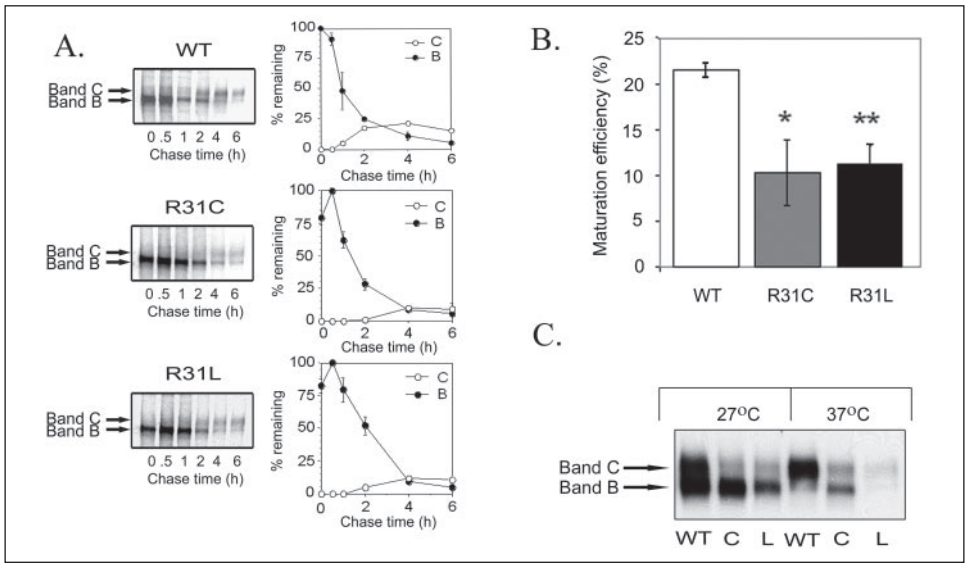

FIGURE 2. **Protein maturation of R31C and R31L CFTR is inefficient compared with wild-type CFTR.** COS-7 cells were pulse-labeled for 30 min at 37 °C with 300 μCi/μl [^{35}S]methionine. After the pulse, radioactive medium was replaced by complete medium, and cells were lysed at the time points indicated. CFTR was immunoprecipitated with 24–1 antibody and analyzed by SDS-PAGE on 6% gels and PhosphorImager analysis (Amersham Biosciences). CFTR maturation efficiency was measured by comparing the maximum density of labeled band B after a 30-min pulse (100%) to the density of band C after 4 h of chase using IPLab software. *A*, representative metabolic labeling experiments are shown for wild type (*WT*), R31C, and R31L (*left panels*). Band B represents the core-glycosylated form of CFTR, and band C represents fully glycosylated protein. The average disappearance of band B (maturation and/or degradation) and formation of band C at each time point are shown (*right panels*). The disappearance of band B (*closed circles*) and formation of band C (*open circles*) were calculated based on densitometry at each time point. Results are plotted as percent of band B at the 0 time point. *B*, summaries of the protein maturation efficiencies for each of the constructs. Maturation efficiencies of wild type, R31C, and R31L were calculated after 4 h of chase (average ± S.D., $n = 3$; *, $p < 0.005$; **, $p < 0.001$). *C*, R31C (*C*) and R31L (*L*) are not temperature-sensitive. *WT*, R31C and R31L CFTR were immunoprecipitated from COS-7 cells 48 h after transfection. 24 h post-transfection, the cells were cultured at either 37 or 27 °C for 24 h before analysis. CFTR was *in vitro* phosphorylated and analyzed by SDS-PAGE and PhosphorImager analysis. A 27 °C incubation increased the amount of B band but did not influence C band production for R31C or R31L CFTR.

RESULTS

The Arg-31 Mutations Inhibit Processing—Because missense mutations in the amino terminus of CFTR often result in processing defects (28) and the Arg-31 mutations were nonconservative substitutions, we first examined the effects of these two changes on the biogenesis of CFTR. Fig. 1 shows the location of the mutations in the context of the CFTR molecule. To examine the maturation efficiency of the Arg-31 mutants, they were expressed in COS-7 cells, and biogenesis tested in metabolic pulse-chase experiments (Fig. 2). For wild-type CFTR, 21.0 ± 1.0% (mean ± S.D.) of the protein was converted from the immature, core-glycosylated form (band B) to the maturely glycosylated protein (band C). This result was consistent with previous reports on the processing of wild-type CFTR in COS-7 cells (22, 29). A significant proportion of band B was converted to band C (17.7 ± 1.5%) by 2 h and was maximal at 4 h after the labeling. With the R31C and R31L mutants, however, very little processing occurred during the first 2 h of chase (0 and 4.7 ± 1.5%, respectively). By 4 h, 10.3 ± 3.0% (R31C) and 11.3 ± 2.1% (R31L) of CFTR was converted to the mature form, indicating that, although there is a processing defect, it does not cause complete inhibition.

Transfected cells were next cultured at 37 or 27 °C to determine whether maturation of the Arg-31 mutants improved at a lower temperature. The results (Fig. 2*C*) indicate that there is no improvement in processing at 27 °C. Overall, the maturation experiments suggest that in contrast to ΔF508 CFTR, compromised processing of the Arg-31 mutations is not the result of a temperature-sensitive folding defect.

The Arg-31 Mutations Have No Effect on Protein Half-life—To determine whether these substitutions affected protein stability, half-lives of the fully processed mutant proteins were measured in metabolic pulse-chase experiments (Fig. 3). The results indicate that the protein half-life of the wild-type protein is 13.3 ± 1.2 h, and the R31C and R31L half-lives are 12.7 ± 0.6 and 14.3 ± 3.1 h, respectively, indicating that,

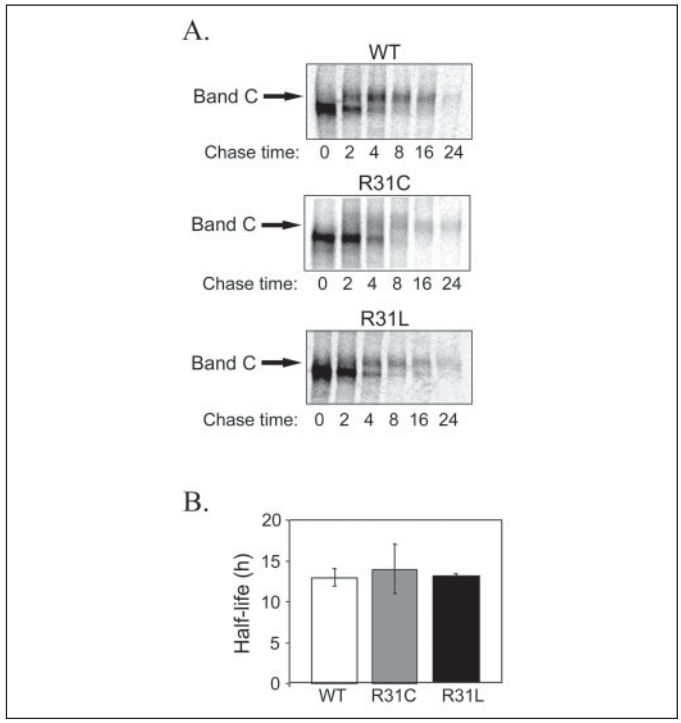

FIGURE 3. **The Arg-31 mutations have a normal protein half-life.** Wild-type, R31C, and R31L CFTR half-lives were determined in COS-7 cells 24 h after transfection. After a 1-h pulse with 300 μCi/μl [^{35}S]methionine-containing medium and the indicated chase periods in complete medium, the cells were lysed in radioimmune precipitation assay buffer, and CFTR was immunoprecipitated using 24–1 antibody. Samples were analyzed by SDS-PAGE and PhosphorImager analysis. *A*, representative gels of wild-type (*WT*), R31C, and R31L CFTR half-lives are shown. The rate of disappearance of band C over time indicates the half-life of the maturely glycosylated protein. *B*, average CFTR protein half-lives were measured by densitometry ($n = 3$).

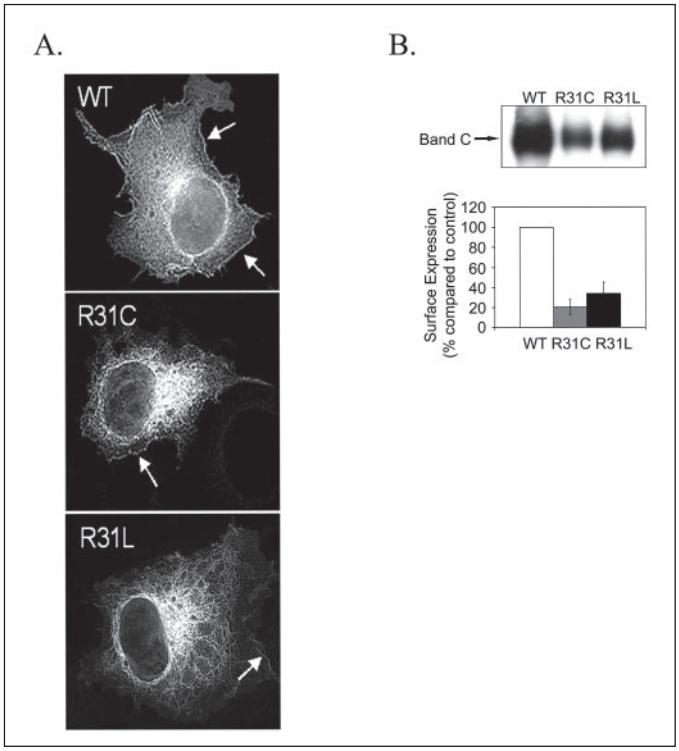

FIGURE 4. **R31C and R31L surface expression is lower than wild-type CFTR.** *A*, wild-type, R31C, and R31L CFTR distributions were examined in COS-7 cells 48 h after transfection using indirect immunofluorescence. Cells were fixed with methanol (−20 °C for 10 min), and CFTR was stained with 24–1 antibody and an anti-mouse Alexa-fluor 596 secondary antibody. *Arrows* indicate the prominant cell surface expression of the wild-type protein CFTR and the diminished amount of surface staining in the R31C and R31L CFTR-expressing cells. *B*, surface expression of CFTR was measured using a surface biotinylation assay. Cell surface proteins were labeled with biotin LC hydrazide. The cells were lysed, CFTR was immunoprecipitated with 24–1, and the samples were analyzed by SDS-PAGE and Western blot. Biotinylated CFTR was detected with horseradish peroxidase-avidin. The average surface expression for each of the constructs is shown below ($n = 4$).

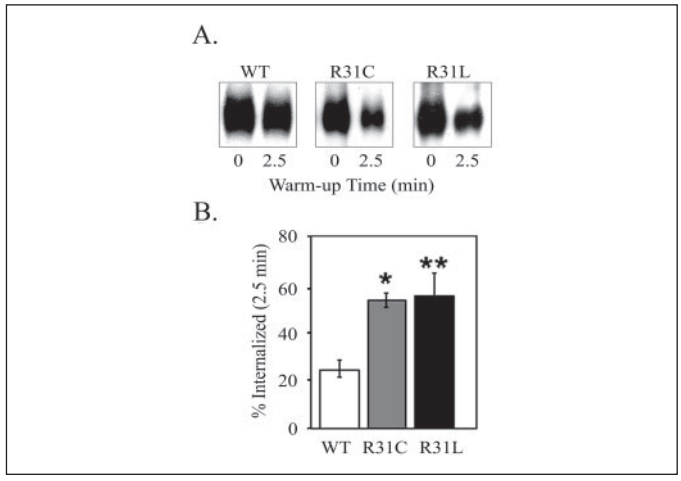

FIGURE 5. **Internalization of the R31C and R31L CFTR mutants is dramatically enhanced compared with the wild-type protein.** *A*, wild-type, R31C, and R31L CFTR internalization in COS-7 cells. COS-7 cells were analyzed 48 h post-transfection for each of the constructs. CFTR internalization was monitored using a two-step cell surface periodate/LC-hydrazide biotinylation procedure (see "Materials and Methods"). At the 0 time points, both steps were conducted at 4 °C to label the entire surface pool of CFTR. Internalization is monitored by a loss of biotinylation of the surface pool by including a 37 °C incubation period (2.5 min) between periodate and biotin LC-hydrazide treatments. After biotinylation, the cells were lysed, and CFTR was immunoprecipitated using the 24–1 antibody. The samples were then analyzed by SDS-PAGE and Western blot. Biotinylated CFTR was detected using horseradish peroxidase-avidin and the 0 and 2.5 min time points for each construct were compared. *B*, summaries are shown for each of the constructs. Internalization was >2-fold faster for both Arg-31 mutants compared with the wild-type protein ($n = 3$, *, $p < 0.001$; **, $p < 0.05$).

although the processing of the mutants was decreased by 50%, the stability of the processed proteins was comparable with wild-type CFTR.

Reduced Surface Expression of R31C and R31L—Because some mutant protein was processed correctly and the protein half-life appeared normal, the surface pool of the Arg-31 mutants was examined next. Wild-type and Arg-31 mutant CFTR intracellular distributions were monitored using indirect immunofluorescence (Fig. 4*A*). For wild-type CFTR, perimeter staining was clearly seen as indicated by the *arrows*. For the R31C and R31L mutants, however, staining was much more restricted to an intracellular, reticular pattern. Perimeter staining was difficult to see in the Arg-31 mutants. To confirm this observation, cells expressing wild-type, R31C, and R31L CFTR were surface-biotinylated (Fig. 4*B*), CFTR was immunoprecipitated, and the biotinylated fraction was detected by Western blot analysis. The results indicate that the surface pool of the R31C and R31L mutants is 20.3 ± 7.5 and 33.6 ± 11.7% of the wild-type protein, respectively ($n = 4$, $p < 0.005$, and $p < 0.05$, respectively. This suggests that the surface pool is smaller than would be predicted based on the biogenesis and half-life experiments.

R31C and R31L Are Internalized More Rapidly than the Wild-type CFTR—Because the surface pool was smaller than predicted, we next tested whether the mutations affected CFTR clearance from the cell surface. To test this, a two-step biotinylation assay was used to monitor CFTR endocytosis during a 2.5-min warm-up period. This period of time is within the linear phase of CFTR endocytosis in these cells (10). The results indicated that 24.8 ± 5.9% of the wild-type protein was internalized in 2.5 min (Fig. 5). This rate of endocytosis was consistent with previous results (12). The R31C and R31L mutants, however, have dramatically altered internalization kinetics with 54 ± 4 and 55 ± 13.9% of the R31C and R31L mutants, respectively (internalized during the same warm-up period). This result suggests these substitutions affect the surface stability of CFTR and are consistent with the lowered surface expression seen with immunofluorescence and surface biotinylation.

The Functional Activity of the R31C and R31L Mutants Is Severely Compromised—As a final measure of the total CFTR chloride channels at the cell surface, we tested the functional activity of the R31C and R31L mutants in two complementary functional assays, macroscopic patch clamp experiments and SPQ assays.

In the first studies, inside-out membrane patches were excised from transfected COS-7 cells using large tip pipettes (3 megohms). CFTR channels were activated with normally saturating concentrations of protein kinase A and MgATP. For cells transfected with wild-type CFTR, the majority of patches (4 of 6) contained many CFTR channels (>30–50) as deduced from the magnitude of the peak currents recorded at ±80 mV (assuming single channel currents of ~0.5 pA; Fig. 6*A*). The recorded currents were determined to be CFTR-mediated on the basis of three criteria: (i) dependence on MgATP, (ii) inhibition by the voltage-dependent pore blocker glibenclamide (30), and (iii) absence from untransfected cells (data not shown). Cells transfected with the R31L and R31C mutants exhibited two differences as compared with wild-type-transfected cells. First, for each mutant the CFTR-mediated currents were much smaller across those patches that exhibited detectable channel activity (Fig. 6, *B* and *C*). Second, cells that were transfected with the mutants exhibited far more silent patches (*i.e.* patches that exhibited no detectable channel activity; see Fig. 6 legend). The silent patches might represent untransfected cells, although the fact that wild-type-transfected cells exhibited very few silent patches makes this less likely. These macroscopic patch clamp results are consistent

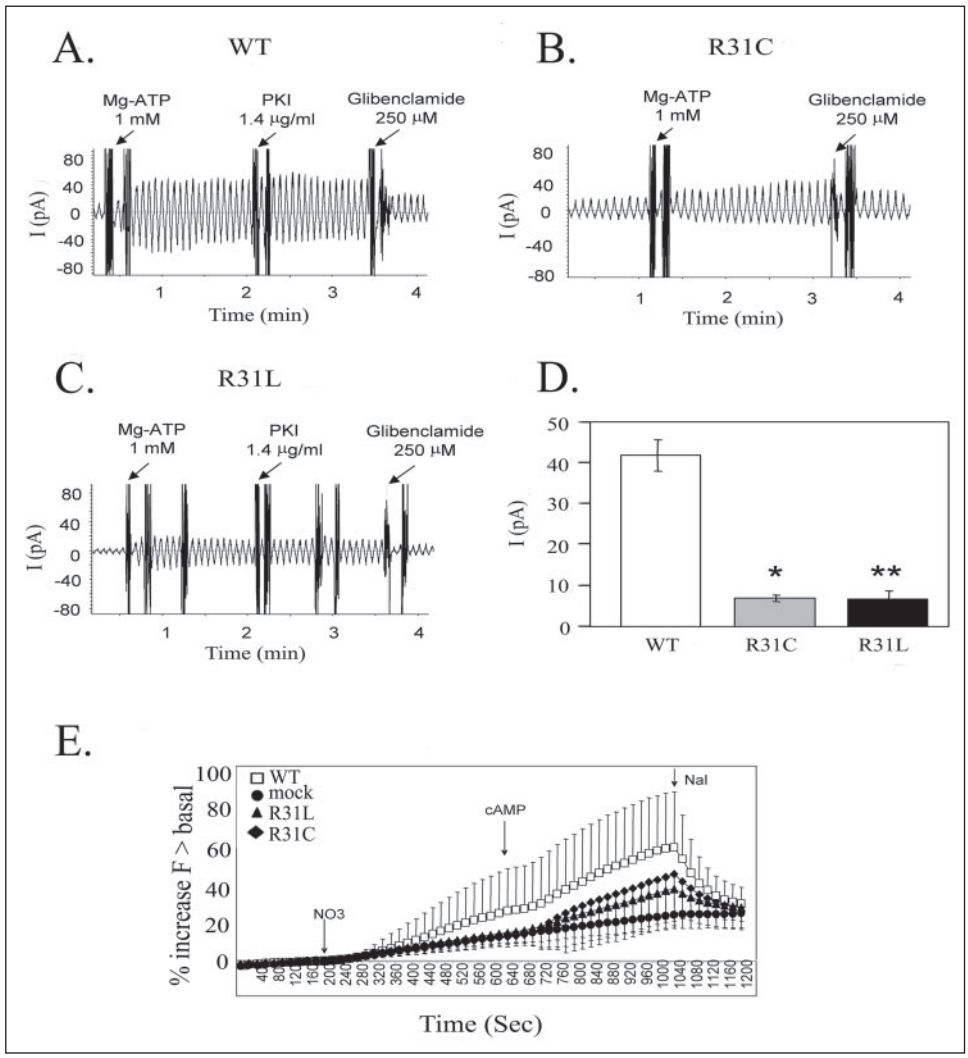

FIGURE 6. **R31C and R31L mutants have diminished channel activity compared with the wild-type protein.** *A–C*, representative current traces for wild-type (*WT*) and R31C and R31L mutants. Macroscopic currents were recorded for membrane patches excised from COS-7 cells transfected with wild-type (*WT*) CFTR or the indicated mutants. The bath contained 110 units/ml protein kinase A. Currents were activated by adding 1 mM MgATP (*first arrow*). Protein kinase A inhibitory peptide (1.4 μg/ml; *PKI*) was added (*second arrow*) to block further phosphorylation. The lack of PKI effect indicates negligible membrane phosphate activity toward CFTR under these conditions. The voltage-dependent pore blocker glibenclamide was added at the end of each experiment. *Vertically centered lines* indicate 0 current levels. *D*, mean glibenclamide-sensitive currents ($\bar{X} \pm$ S.E.) recorded at −80 mV for each construct ($n = 4$ patches each). Note that the data for the L and C mutants overestimate their functional activities, because unlike WT, most excised mutant patches exhibited undetectable CFTR activity and were excluded from this analysis (R31L, 4 active patches of 13 total; R31C, 4 active patches of 19 total; wild type, 4 active patches of 6 total). *, $p < 0.001$; **, $p < 0.01$. *E*, functional analysis of wild-type and R31C and R31L CFTR using SPQ fluorescence. The change in SPQ fluorescence is shown for COS-7 cells expressing wild-type, R31C, and R31L CFTR. Cells were stimulated with 20 μM forskolin (at *arrow*, cyclic AMP (*cAMP*)). The change in SPQ fluorescence was significantly more than for the negative control (*mock*-transfected cells), but substantially lower than for the wild-type protein. Curves were generated from the mean ± S.D. of cells studied over 3 days ($n = 120$ cells/condition; top 90% of all cells studies as described under "Material and Methods"). The wild-type CFTR sample had significantly higher iodide flux (in the presence of forskolin) than the Arg-31 mutants or mock sample ($p < 0.001$ by χ^2 test for each condition compared with wild-type CFTR).

with the notion that the Arg-31 mutations reduce the steady-state surface expression of CFTR. As with any macroscopic functional assay, however, these findings do not exclude the possibility that the Arg-31 mutations also affect the single channel properties of CFTR.

In the second functional analyses, the Arg-31 mutants were tested using an SPQ halide efflux protocol to measure anion transport through the cell surface membrane. Fig. 6*E* shows that, in wild-type CFTR-expressing cells, halide transport was activated after stimulation with cyclic AMP agonists (20 μM forskolin and 100 μM 3-isobutyl-1-methlyxanthine). Analysis of the Arg-31 mutants, however, revealed that the halide transport activities were reduced compared with the wild-type protein. This result, in combination with the patch clamp analysis, supports the biochemical data and indicates that there is a decrease in the functional chloride channels at the surface in cells expressing the Arg-31 mutants compared with the wild-type controls.

DISCUSSION

The R31C and R31L are naturally occurring missense CF mutations that appear to have a mild phenotype (31).[3] Both of these mutations are rare (identified once in 284 CF chromosomes, for the R31L mutation). The R31C mutation was found in a 45-year-old male CF patient diagnosed in childhood who was pancreatic-sufficient with moderate pulmonary symptoms and a positive sweat test. His other allele is the I556V mutation. The R31L was found in a 24-year-old female CF patient who was pancreatic-sufficient with normal lung function but a positive sweat test. The other allele was not identified. Based on these descriptions, both mutations appear to be associated with mild disease, and our biochemical and functional data support this idea, because there is some surface-expressed and functional chloride channel activity associated with these mutants.

The analysis of the Arg-31 CFTR suggests that replacement of the arginine with either cysteine or leucine at position 31 affects protein biogenesis. The biogenesis defect is not complete, however, because some CFTR is processed properly and reaches the cell surface. Interestingly, not only was biogenesis compromised by ~50%, the kinetics of transport from the endoplasmic reticulum to the Golgi apparatus as assessed by glycosylation changes appeared slower for the two mutants, particularly at the 2-h time point. By 6 h, however, there was a decrease in the amount of labeled band C for both of the mutants compared with earlier time points. Surprisingly, once the protein was fully processed, the stability of the Arg-31 mutants was comparable with the wild-type protein.

The fact that these substitutions affect biogenesis is not surprising, given that, in the Cystic Fibrosis Mutation Data Base, there are 27 missense mutations that have been identified within the 80-residue amino-terminal tail.[3] Furthermore, our own studies using deletion analysis have shown that the amino terminus is essential for CFTR protein processing (10, 32). One possible reason for the critical nature of the amino

terminus is that this region has been shown to control protein kinase A-dependent channel gating through a physical interaction with the distal region of nucleotide binding domain 1 and the R domain (residues 595–823) (33). Furthermore, alanine scanning of this region shows that a number of sites are critical for processing (32), suggesting that point mutations in this region of the molecule are poorly tolerated, even when the substitutions are alanine residues. In the case of the Arg-31 mutations, the substitutions are nonconservative, and based on the data, these nonconservative changes affect CFTR processing.

The reason these two mutations affect endocytosis is unclear. One intriguing possibility, however, is that they introduce potential internalization signals in the amino terminus of CFTR, $Y^{28}XXC^{31}$ and $Y^{28}XXL^{31}$. With the introduction of the hydrophobic residue at position 4, they conform to a consensus internalization signal that consists of $YXX\Phi$, where Φ is a large hydrophobic residue and X is any residue (13). Whether these mutations are recognized by the endocytic machinery of the cell, however, cannot be determined from the present studies. In fact, it is possible that these mutations somehow affect the recognition of the tyrosine-based signal in the carboxyl terminus and promote enhanced endocytosis. A third possibility is that the mutations alter the tertiary structure of CFTR and this influences the rate of clearance of CFTR from the cell surface. However, if the structure were dramatically altered, then the protein half-life might be affected, and this is certainly not the case with these particular mutations.

Another CFTR mutation was recently identified in the second intracellular loop, N287Y, which affects endocytosis over wild-type levels (34). Interestingly, the N287Y mutation does not introduce a consensus tyrosine-based signal and did not affect biogenesis of CFTR. This suggests that overactive internalization alone is sufficient to promote a disease phenotype (34). In the case of the Arg-31 mutants, a combination of a biogenesis defect coupled with enhanced endocytosis results in a decrease in the functional amount of CFTR at the cell surface. The mild phenotype of patients harboring these mutations is consistent with the residual amount of activity of the mutants found in this study.

The altered surface stability defect in the Arg-31 mutants without a corresponding defect in protein stability is in contrast to the ΔF508 mutation. ΔF508 is a class II mutation that misfolds during biogenesis and is rapidly degraded by the endoplasmic reticulum-associated degradation pathway (35). ΔF508, however, is a temperature-sensitive mutation (18), and some CFTR escapes endoplasmic reticulum-associated degradation when cells are cultured at 27 °C. Recent studies on rescued ΔF508 CFTR in airway epithelia indicate that, similar to the Arg-31 mutants, ΔF508 CFTR is also more rapidly internalized than the wild-type protein (19). The Arg-31 mutants do have a partial biogenesis defect, indicating their status as class II mutations. However, culturing at 27 °C has no effect on Arg-31 mutant biogenesis, indicating that they are not temperature-sensitive. Analysis of the ΔF508, N287Y, and R31L and R31C indicate that alterations in the transport of CFTR at the cell surface, whether it is enhanced internalization or compromised recycling, can result in a disease phenotype.

In summary, two naturally occurring mutations in the amino-terminal cytoplasmic tail of CFTR at position 31 dramatically enhance endocytosis. This, in combination with a partial biogenesis defect, leads to diminished chloride channel activity at the cell surface and explains two of the cellular defects observed in these mutations.

Acknowledgments—We thank David McPerson and the University of Alabama at Birmingham Molecular Biology Core Facility for preparation of the Arg-31 mutants.

REFERENCES

1. Prince, L. S., Workman, R. B., Jr., and Marchase, R. B. (1994) *Proc. Natl. Acad. Sci. U. S. A.* **91,** 5192–5196
2. Lukacs, G. L., Segal, G., Kartner, N., Grinstein, S., and Zhang, F. (1997) *Biochem. J.* **328,** 353–361
3. Bradbury, N. A., Cohn, J. A., Venglarik, C. J., and Bridges, R. J. (1994) *J. Biol. Chem.* **269,** 8296–8302
4. Lukacs, G. L., Chang, X., Kartner, N., Rotstein, O. D., Riordan, J. R., and Grinstein, S. (1992) *J. Biol. Chem.* **267,** 14568–14572
5. Prince, L. S., Tousson, A., and Marchase, R. B. (1993) *Am. J. Physiol.* **264,** C491–C498
6. Webster, P., Vanacore, L., Nairn, A. C., and Marino, C. R. (1994) *Am. J. Physiol.* **267,** C340–C348
7. Demolombe, S., Baro, I., Laurent, M., Hongre, A. S., Pavirani, A., and Escande, D. (1994) *Eur. J. Cell Biol.* **65,** 214–219
8. Biwersi, J., and Verkman, A. S. (1994) *Am. J. Physiol.* **266,** C149–C156
9. Gentzsch, M., Chang, X. B., Cui, L., Wu, Y., Ozols, V. V., Choudhury, A., Pagano, R. E., and Riordan, J. R. (2004) *Mol. Biol. Cell* **15,** 2684–2696
10. Prince, L. S., Peter, K., Hatton, S. R., Zaliauskiene, L., Cotlin, L. F., Clancy, J. P., Marchase, R. B., and Collawn, J. F. (1999) *J. Biol. Chem.* **274,** 3602–3609
11. Hu, W., Howard, M., and Lukacs, G. L. (2001) *Biochem. J.* **354,** 561–572
12. Peter, K., Varga, K., Bebok, Z., McNicholas-Bevensee, C. M., Schwiebert, L., Sorscher, E. J., Schwiebert, E. M., and Collawn, J. F. (2002) *J. Biol. Chem.* **277,** 49952–49957
13. Collawn, J. F., Stangel, M., Kuhn, L. A., Esekogwu, V., Jing, S., Trowbridge, I. S., and Tainer, J. A. (1990) *Cell* **63,** 1061–1072
14. Weixel, K. M., and Bradbury, N. A. (2000) *J. Biol. Chem.* **275,** 3655–3660
15. Weixel, K. M., and Bradbury, N. A. (2001) *Pfluegers Arch.* **443,** Suppl. 1, S70–S74
16. Weixel, K. M., and Bradbury, N. A. (2001) *J. Biol. Chem.* **276,** 46251–46259
17. Rowntree, R. K., and Harris, A. (2003) *Ann. Hum. Genet.* **67,** 471–485
18. Denning, G. M., Anderson, M. P., Amara, J. F., Marshall, J., Smith, A. E., and Welsh, M. J. (1992) *Nature* **358,** 761–764
19. Swiatecka-Urban, A., Brown, A., Moreau-Marquis, S., Renuka, J., Coutermarsh, B., Barnaby, R., Karlson, K. H., Flotte, T. R., Fukuda, M., Langford, G. M., Stanton, B. A., (2005) *J. Biol. Chem.* **280,** 36762–36772
20. Wang, W., Li, G., Clancy, J. P., and Kirk, K. L. (2005) *J. Biol. Chem.* **280,** 23622–23630
21. Sharma, M., Pampinella, F., Nemes, C., Benharouga, M., So, J., Du, K., Bache, K. G., Papsin, B., Zerangue, N., Stenmark, H., and Lukacs, G. L. (2004) *J. Cell Biol.* **164,** 923–933
22. Varga, K., Jurkuvenaite, A., Wakefield, J., Hong, J. S., Guimbellot, J. S., Venglarik, C. J., Niraj, A., Mazur, M., Sorscher, E. J., Collawn, J. F., and Bebok, Z. (2004) *J. Biol. Chem.* **279,** 22578–22584
23. Straley, K. S., Daugherty, B. L., Aeder, S. E., Hockenson, A. L., Kim, K., and Green, S. A. (1998) *Mol. Biol. Cell* **9,** 1683–1694
24. Bebok, Z., Varga, K., Hicks, J. K., Venglarik, C. J., Kovacs, T., Chen, L., Hardiman, K. M., Collawn, J. F., Sorscher, E. J., and Matalon, S. (2002) *J. Biol. Chem.* **277,** 43041–43049
25. Cheng, S. H., Rich, D. P., Marshall, J., Gregory, R. J., Welsh, M. J., and Smith, A. L. (1991) *Cell* **66,** 1027–1036
26. Clancy, J. P., Ruiz, F. E., and Sorscher, E. J. (1999) *Am. J. Physiol.* **276,** C361–C369
27. Clancy, J. P., Hong, J. S., Bebok, Z., King, S. A., Demolombe, S., Bedwell, D. M., and Sorscher, E. J. (1998) *Biochemistry* **37,** 15222–15230
28. Cormet-Boyaka, E., Jablonsky, M., Naren, A. P., Jackson, P. L., Muccio, D. D., and Kirk, K. L. (2004) *Proc. Natl. Acad. Sci. U. S. A.* **101,** 8221–8226
29. Cheng, S. H., Gregory, R. J., Marshall, J., Paul, S., Souza, D. W., White, G. A., O'Riordan, C. R., and Smith, A. E. (1990) *Cell* **63,** 827–834
30. Schultz, B. D., DeRoos, A. D., Venglarik, C. J., Singh, A. K., Frizzell, R. A., and Bridges, R. J. (1996) *Am. J. Physiol.* **271,** L192–L200
31. Zielenski, J., Markiewicz, D., Chen, H. S., Schappert, K., Seller, A., Durie, P., Corey, M., and Tsui, L. C. (1995) *Hum. Mutat.* **5,** 43–47
32. Naren, A. P., Quick, M. W., Collawn, J. F., Nelson, D. J., and Kirk, K. L. (1998) *Proc. Natl. Acad. Sci. U. S. A.* **95,** 10972–10977
33. Naren, A. P., Cormet-Boyaka, E., Fu, J., Villain, M., Blalock, J. E., Quick, M. W., Kirk K. L. (1999) *Science* **286,** 388–389
34. Silvis, M. R., Picciano, J. A., Bertrand, C., Weixel, K., Bridges, R. J., and Bradbury, N. A. (2003) *J. Biol. Chem.* **278,** 11554–11560
35. Ward, C. L., Omura, S., and Kopito, R. R. (1995) *Cell* **83,** 121–127

Mutations in the Amino Terminus of the Cystic Fibrosis Transmembrane Conductance Regulator Enhance Endocytosis

Asta Jurkuvenaite, Karoly Varga, Krzysztof Nowotarski, Kevin L. Kirk, Eric J. Sorscher, Yao Li, John P. Clancy, Zsuzsa Bebok and James F. Collawn

J. Biol. Chem. 2006, 281:3329-3334.
doi: 10.1074/jbc.M508131200 originally published online December 8, 2005
